Environmental Earth Sciences (2025) 84:355
https://doi.org/10.1007/s12665-025-12258-5

ORIGINAL ARTICLE

Performance of remotely sensed precipitation products in capturing meteorological drought over typical agricultural planting area

Pengnian Huang[1] · Manjie Huang[1] · Aiqing Feng[2,6] · Yanzhong Li[1,5] · Kunxia Yu[3] · Yintong Guo[4] · Wenjun Yu[1] · Kang Yang[1]

Received: 13 October 2024 / Accepted: 12 April 2025

Abstract
Remote sensed precipitation products (RSPPs) can provide reliable data for drought monitoring. However, using numerous RSPPs can introduce significant uncertainties due to their discrepancies. This study focuses on the Huang-Huai-Hai Plain in China, a key agricultural region sensitive to meteorological drought. Using grid precipitation interpolated by observed data from the China Meteorological Administration (CMA), we evaluated the performance of three long-term series (> 30 years) RSPPs (PERSIANN-CDR, CHIRPS, and MSWEP) in capturing the spatial and temporal characteristics of meteorological drought events. We found that (1) three RSPPs can generally reproduce the pattern of annual precipitation, but they are difficult to accurately capture the trend of CMA. (2) MSWEP performs better than the other two products in identifying drought variation and area proportions at various spatiotemporal scales, with the one-month scale (SPI1) being the optimal timescale for RSPPs to identify meteorological drought. (3) All RSPPs can reproduce the pattern of drought categories and characteristics, with their performance order of MSWEP > CHIRPS > PERSIANN-CDR. This indicates considerable room for improvement in depicting the drought characteristics. Our results can guide the selection of the RSPPs for meteorological drought monitoring and disaster avoidance.

Keywords Remote sensing precipitation products · SPI · Drought characteristics · Run theory · Huang-Huai-Hai Plain

Introduction

Drought is one of the most catastrophic natural disasters (Gimeno-Sotelo et al. 2024). It is typically caused by prolonged water shortage due to insufficient precipitation, and it can lead to significant losses to agricultural production, domestic water supply, ecosystem stability, and socioeconomic development (Yuan et al. 2023; Zhang et al. 2023; Xie et al. 2024). In 2022, an unprecedented drought caused by a prolonged precipitation deficit affected the Yangtze River Basin, leading to severe electric power shortages, reduced production on 4.08 million hectares of farmland, and a lack of fresh water for 4.3 million people and 0.35 million livestock (Ma and Yuan 2023). Therefore, monitoring droughts caused by precipitation shortage is crucial for drought early warning, prevention, and disaster reduction.

Drought indicators are crucial tools for monitoring drought, and many of them have been widely used in practical applications. Examples include the Palmer Drought Severity Index (PDSI), Rainfall Deciles (RD), Surface Water and Supply Index (SWSI), Standardized Precipitation

✉ Aiqing Feng
fengaq@cma.gov.cn

1 School of Hydrology and Water Resources, Nanjing University of Information Science and Technology, Nanjing 210044, China

2 China Meteorological Administration Key Laboratory for Climate Prediction Studies, National Climate Center, Beijing 100081, China

3 State Key Laboratory of Eco-Hydraulics in Northwest Arid Region, Xi'an University of Technology, Xi'an 710048, China

4 Ocean and Earth Science, University of Southampton, Southampton SO14 7BL, UK

5 National Key Laboratory of Water Disaster Prevention, Hohai University, Nanjing 210024, China

6 Hydro-Environmental Research Centre, School of Engineering, Cardiff University, Cardiff CF24 3AA, UK

Published online: 11 June 2025

Index (SPI), etc. (Zargar et al. 2011). Among these indicators, the calculation of SPI is based on the assumption that precipitation plays a decisive role in drought. Since it only requires precipitation as an input, it can effectively reduce the uncertainties caused by multiple data inputs and represent the deficit and surplus of precipitation (McKee et al. 1993). Furthermore, SPI has the advantages of simple calculation and a flexible time scale. Nowadays, SPI has been frequently applied for monitoring meteorological droughts and early warnings at different spatial and temporal scales (Brito et al. 2021; Su et al. 2018; Li et al. 2022b; Gimeno-Sotelo et al. 2024).

When using SPI to monitor drought, the accuracy of input precipitation largely determines the reliability of drought characteristics (Guo et al. 2022). Various precipitation data can be used to calculate SPI, such as gauge-based observation, radar-based observation, and remote sensing-based precipitation products (RSPPs). Scientific communities argue that the gauge-based values can be considered the actual value of precipitation. However, gauge observation is easily affected by complex terrain and other factors, and the observation stations are sparse and uneven, especially in remote and inaccessible areas. Accurately capturing precipitation patterns using limited data is difficult. In contrast, RSPPs have numerous advantages, such as quasi-global coverage, near-real-time, and high spatiotemporal resolution (Li et al. 2024; Sreeparvathy and Srinivas 2022), providing highly accurate precipitation estimates. However, there are currently dozens of popular RSPPs available (Sun et al. 2018), such as the Precipitation Estimation from Remotely Sensed Information Using Artificial Neural Networks-Climate Data Record (PERSIANN-CDR) products (Ashouri et al. 2015), Climate Hazards Group Infrared Precipitation with Stations (CHIRPS) products (Funk et al. 2015), Multi-Source Weighted-Ensemble Precipitation (MSWEP) products (Beck et al. 2019), Climate Prediction Center morphing technique (CMORPH) products (Joyce et al. 2004), and the Integrated Multi-satellite Retrievals for GPM (IMERG) products (Huffman et al. 2015), etc. These RSPPs have been widely used in meteorological drought detection (AghaKouchak et al. 2015).

Many researchers have conducted a series of comparisons to assess the skill of multi-source RSPPs in drought detection. For example, Guo et al. (2017) found that CHIRPS has excelled in capturing drought evaluation in the Mekong River, particularly skillful at the 3-month time scale. In comparison, Li et al. (2022a) found that MSWEP effectively depicts drought characteristics in typical watersheds in Central Asia; Zhong et al. (2019) found that among PERSIANN-CDR, CHIRPS, and TMPA3B42, TMPA3B42 has the best drought monitoring performance in China; Liu et al. (2019) evaluated CHIRPS and MSWEP in the Tibetan Plateau region, finding CHIRPS is more suitable for more minor spatial scales due to its high spatial resolution and effective characterization of detailed features. These RSPPs exhibit varying skills in capturing the drought characteristics across different regions, making it necessary to evaluate their applicability before employing them in drought monitoring.

In addition to the performance discrepancies between different RSPPs, their data lengths also vary. Generally, most RSPPs have short time series (< 20 years). However, the World Meteorological Organization (WMO) recommends a time series of at least 30 years or more for drought monitoring, limiting the widespread use of shorter time series. To our knowledge, three typical RSPPs have time series spanning more than 30 years, including MSWEP, PERSIANN-CDR, and CHIRPS. However, their performance requires further verification.

Moreover, the drought monitoring performance of RSPPs is relatively weak in climate change-sensitive and major grain-producing areas. The Huang-Huai-Hai Plain is a crucial grain production region in China, and the main economic crops include corn, wheat, soybeans, peanuts, etc. (Liu et al. 2010). Frequent drought occurrences have significantly reduced crop yield (Tuan et al. 2011). Therefore, using observational gridded precipitation data (CMA) from 1983 to 2019 as a reference, we evaluate the performance of three long-term series (> 30a) of RSPPs (PERSIANN-CDR, CHIRPS, and MSWEP) in monitoring drought events in the Huang-Huai-Hai Plain. Our study aims to answer three scientific questions: (1) Can the three long-term RSPPs capture the spatiotemporal precipitation pattern of CMA in the Huang-Huai-Hai Plain of China? (2) How do the three RSPPS reproduce the SPI at different time scales? (3) What are the differences among the three RSPPs in assessing drought categories and characteristics? The answers to these questions will provide great guidance for selecting and improving the RSPPs for meteorological drought monitoring in the Huang-Huai-Hai Plain, and provide scientific reference for agricultural drought preparation and mitigation.

Study area and datasets

Study area

The Huang-Huai-Hai Plain is located in central and eastern China (30°–42° N, 110°–125° E), including Beijing, Tianjin, Hebei Province, Henan Province, and Shandong Province (Fig. 1). This region is one of China's nine major grain production areas. The multi-year average temperature ranges from 10 to 15 °C, with annual precipitation of 500–1000 mm. The average annual evaporation is 897–913 mm, resulting in intense evaporation in the field.

Fig. 1 Location of the Huang-Huai-Hai Plain

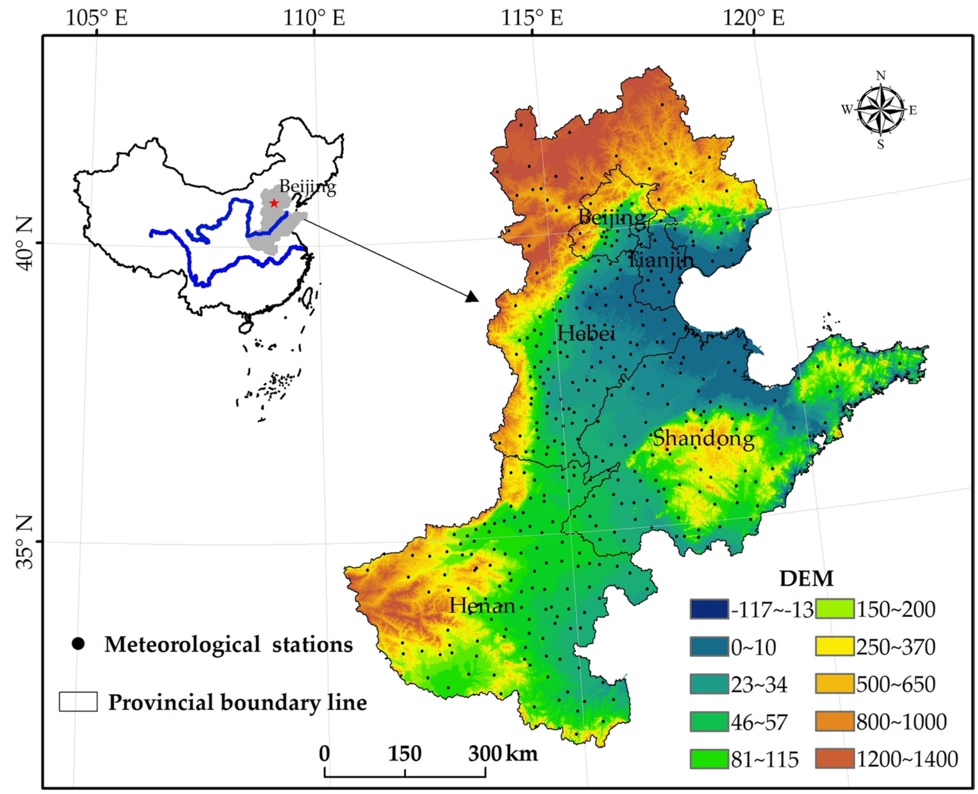

Precipitation datasets

Observational precipitation

The daily precipitation data from 395 meteorological stations were obtained from the National Meteorological Information Center. These observation data have undergone strict quality control, including checks for climate, stations, and region outliers, as well as internal, temporal, and spatial consistency, covering the period from 1960 to 2022. For the performance evaluation, stations were selected based on the following criteria: the missing data does not exceed 0.5% and 5% for the whole study period and any given year. The results show that 345 stations met these requirements, and their spatial distribution pattern is depicted in Fig. 1. Missing records were replaced by climatological averages for the same calendar day at a given station. We applied the professional spatial interpolation software Anusplin, which utilizes thin-plate spline functions to construct interpolation surfaces. By minimizing the overall curvature of the interpolation function, Anusplin can effectively smooth precipitation or temperature data across complex terrains, such as areas with significant topographical variation (Hutchinson and Xu 2004). The daily precipitation data were interpolated to a $0.05° \times 0.05°$ grid, and the monthly precipitation was derived by aggregating the daily averages.

Remote sensed precipitation products (RSPPs)

Three long-term remote sensed precipitation products (RSPPs) were selected for our study, including PERSIANN-CDR, CHIRPS v2.0, and MSWEP v2.0, which will be shortened for PERSIANN-CDR, CHIRPS, and MSWEP. Specifically, PERSIANN-CDR is a precipitation dataset with the advantages of a long time series and global coverage. It has been widely used to investigate precipitation fluctuations caused by climate change, particularly extreme events (Ashouri et al. 2015), with a time span from 1983 to the present. CHIRPS couples high-resolution remote sensing information with ground observation data, offering advantages of short delay, high spatiotemporal resolution, slight bias, and long time series. This dataset has been widely applied in climate change analysis, extreme drought early warning and monitoring, and flood simulation (Funk et al. 2015). MSWEP combines the strengths of ground observations, remote sensing information, and reanalysis datasets to provide a near-true estimate of global precipitation (Beck et al. 2019). These three products were selected for comparison mainly to investigate the performance of RSPPs with different spatial resolutions, remote sensing sensors, and retrieval methods in capturing meteorological drought. The time span was unified from 1983 to 2019. To keep spatiotemporal consistency of all RSPPs, the spatial resolution of the three RSPPs was resampled to a 0.05°×0.05° grid using the bilinear interpolation method (Table 1).

Methodology

Basic statistical metrics

To comprehensively assess the skill of three typical RSPPs in capturing meteorological drought in the Huang-Huai-Hai plain, we selected four statistical metrics, including relative bias (rBIAS), root mean square error (fRMSE), and correlation coefficient (r) and Kling-Gupta coefficient (KGE). The equations are shown as follows.

$$fRMSE = \frac{\sqrt{\frac{1}{N}\sum_{i=1}^{N}(R_i - G_i)}}{\frac{1}{N}\sum_{i=1}^{N}G_i} \tag{1}$$

$$r = \frac{\sum_{i=1}^{N}(R_i - \overline{R_i})(G_i - \overline{G_i})}{\sqrt{\sum_{i=1}^{N}(R_i - \overline{R_i})^2}\sqrt{\sum_{i=1}^{N}(G_i - \overline{G_i})^2}} \tag{2}$$

$$aBIAS = \frac{\sum_{i=1}^{N}R_i - G_i}{N} \tag{3}$$

$$rBIAS = \frac{\sum_{i=1}^{N}R_i - G_i}{\sum_{i=1}^{N}G_i} \times 100\% \tag{4}$$

$$KGE = 1 - \sqrt{(1-r)^2 + (1 - \frac{\sigma_R}{\sigma_G})^2 + (1 - \frac{\mu_R}{\mu_G})^2} \tag{5}$$

where G_i and R_i represent the observational and remote sensing-based precipitation estimates, respectively. σ_G and μ_G are the average and standard error of the observational precipitation, respectively. σ_R and μ_R are the mean and standard error of precipitation estimated by RSPPs, respectively.

Meteorological drought index of SPI and classification

SPI is used to characterize the probability of precipitation events occurring over a specific time period, and it can describe and compare drought phenomena across different climate regions (Sternberg et al. 2011). Since SPI uses precipitation as the sole input, it can reduce uncertainties caused by other factors, such as temperature and wind. This indicator allows us to focus on the performance of precipitation in reproducing the meteorology drought. Drought is classified into four classifications using the SPI values, as shown in Table 2.

Categorical probability skill

We selected three statistical indicators to quantify the capability of RSPPs in detecting drought categories: probability of detection (POD), critical success index (CSI), and Heidke skill score (HSS). Specifically, POD measures the probability of correctly detecting drought events, representing the rate of successful detection (Ebert et al. 2007). CSI refers to the probability of successful drought monitoring (Schaefer-forecasting 1990). HSS is a standard performance metric for assessing classification skills (Wilks 2011), depicting the percentage of months RSPPs correctly capture drought category events as of all drought months. In our study, an SPI value of < -1 was the threshold value for identifying a drought event for calculating POD and CSI. HSS used – 1,

Table 2 SPI classification

Drought classification	SPI value
Near normal	(– 1, 0)
Moderate drought	(– 1.5, – 1.0]
Severe drought	(– 2.0, – 1.5]
Extreme drought	(– ∞, – 2]

Table 1 Summary of the three long-term RSPPs and CMA used in the study

Name	Temporal Range	Temporal Resolution	Spatial Cover age	Spatial Resolution
PERSIANN - CDR	1983 - Now	Daily	60°N ~ 60°S	0.25
CHIRPS v2.0	1981 - Now	Daily	50°N ~ 50°S	0.05
MSWEP v2.0	1979 - Now	3 h	Global	0.1

– 1.5, and – 2 of SPI to define moderate drought, severe drought, and extreme drought, respectively. The higher the POD, CSI, and HSS values, the better the products' capability to detect drought characteristics.

$$POD = \frac{N(R_i = 1\&G_i = 1)}{N(G_i = 1)} \times 100 \tag{6}$$

$$CSI = \frac{N(R_i = 1\&G_i = 1)}{N(G_i = 1) + N(R_i = 1\&G_i = 0)} \times 100 \tag{7}$$

$$HSS = \frac{N(R_i = 1\&G_i = 1) - N(E_i)}{N(G_i = 1) - N(E_i)} \times 100 \tag{8}$$

$R_i = 1$ ($R_i = 0$) and $G_i = 1$ ($G_i = 0$) represent the number of drought events in the month i correctly (or incorrectly) detected by RSPPs and CMA, respectively. E_i represents the expected number of classified drought events in the month i that are correctly detected by chance.

Run theory and drought event characteristics

The run theory is applied to detect drought events in our study. If the SPI of certain months is below the threshold, these months are classified as drought months (Fleig et al. 2006; Li et al. 2022b). This study defines a drought event primarily as SPI ≤ – 0.5 lasting more than two months. However, an exception is made for high-intensity short-term droughts: if a drought event lasts only one month but has a severity of SPI ≤ – 1.5, it is also considered a valid drought event. This adjustment ensures that extremely intense but short-lived droughts are not overlooked in the analysis. We employ three indices to test the capability of the three long-term RSPPs in detecting drought events. They are mean drought event duration (MDD), mean drought event severity (MDS), mean drought event intensity (MDI), and mean drought event peak. (MDP). The calculation formulas are as follows.

$$MDD = \frac{\sum_{i=1}^{n} DD_i}{N} \tag{9}$$

$$MDS = \frac{\sum_{i=1}^{n} DS_i}{N}, \ DS = \sum_{j=1}^{DD} \left|SPI_j\right| \tag{10}$$

$$MDI = \frac{\sum_{i=1}^{N} DI_i}{N}, DI = \frac{DS}{DD} \tag{11}$$

$$MDP = \frac{\sum_{i=1}^{N} DP_i}{N}, DP = \max_{1 \le j \le DD} \left|SPI_{\mathrm{j}}\right| \tag{12}$$

where DD, DS, DI, and DP are the duration period, cumulative value, intensity value, and peak value of SPI for a drought event, respectively. The i is the ith drought event, and j is the index of the drought month in a specific drought event.

Results

Basic skill of RSPPs

Mean and trend patterns of precipitation

Figure 2 presents the spatial distribution of mean annual precipitation and trends of CMA and three RSPPs during 1983–2019. The mean annual precipitation presents a gradually decreasing distribution from southeast to northwest in our study area (Fig. 2a). Three RSPPs generally captured the spatial pattern of the mean annual precipitation. However, they all slightly overestimated the true values of CMA. PERSIANN-CDR, CHIRPS, and MSWEP overestimated the mean annual precipitation by 6.0%, 3.6%, and 3.6%, respectively. Compared with the other two products, the PERSIANN-CDR shows a smoother spatial distribution pattern, but it has obvious shortcomings in accurately capturing the local precipitation pattern. For example, it significantly overestimates the low precipitation information in the mountainous areas in the northwest region (Fig. 2b).

For the spatial distribution of multi-year precipitation trends, 53.3% of the area showed a decreasing trend, reaching – 0.09 mm/a^2 (Fig. 2e). It is difficult for the three RSPPs to accurately capture the trend of CMA, with significant spatial discrepancies in their performance. For example, compared to CMA, the trend is significantly underestimated by MSWEP in most areas of Henan and Shandong provinces (Fig. 2h). The bias in MSWEP led to a severe underestimate of the annual precipitation trend by 1.85 mm/a^2. CHIRPS significantly over-estimates the precipitation trend by 2.44 mm/a^2, especially in central and western Shandong province (Fig. 2g). PERSIANN-CDR overestimates the precipitation trend in the study area as a whole, reaching 0.44 mm/a^2 (Fig. 2f). Overall, while all three RSPPs can reasonably reproduce the spatial pattern of multi-year mean precipitation, but none of them can accurately capture the pattern of precipitation trends.

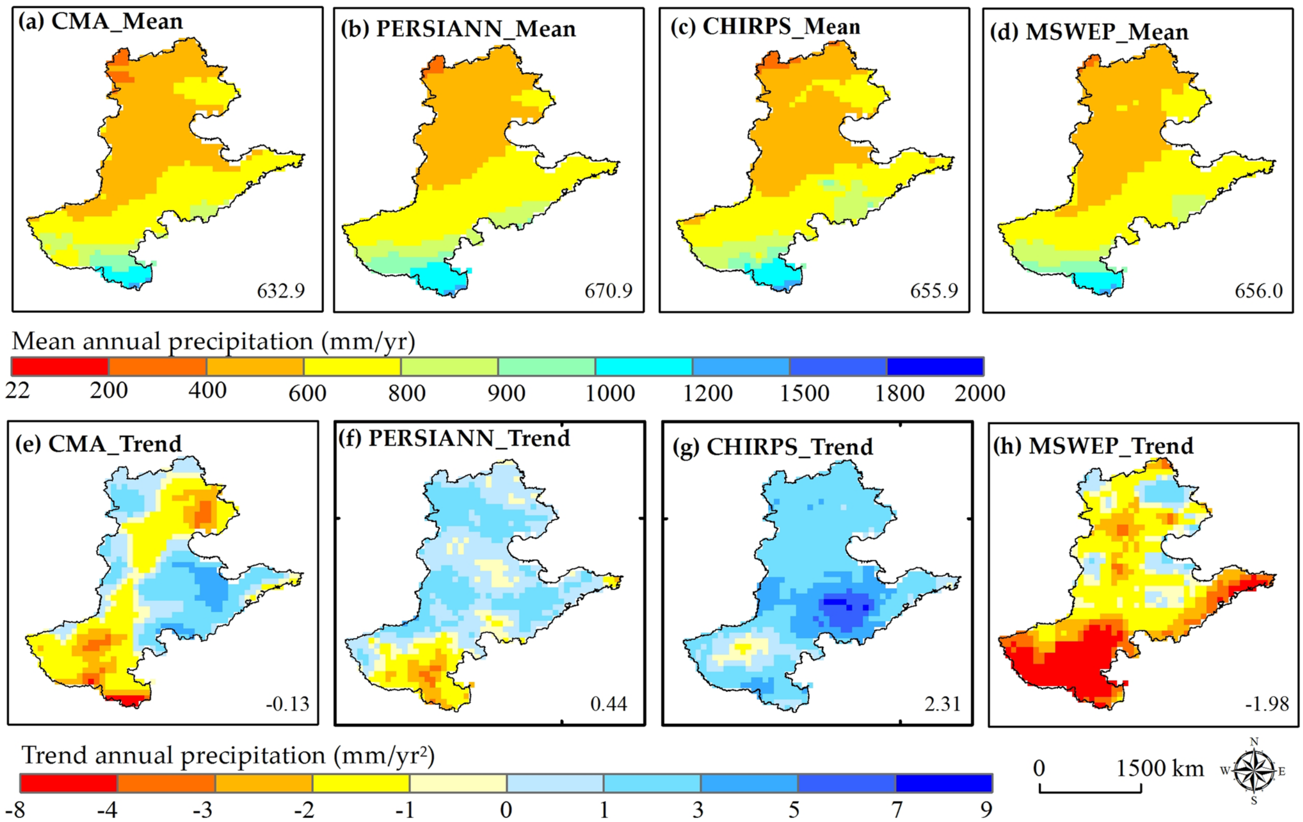

Fig. 2 The spatial distribution of mean and trend values of CMA and three RSPPs during 1983–2019

Basic statistical performance

Figure 3 presents the spatial distribution of the basic statistical performance of different RSPPs. For rBIAS, the three RSPPs overestimated the observational values of CMA, with the overestimation by 5.93%, 3.45%, and 3.98% (Fig. 3a–c). The performance of CHIRPS and MSWEP is acceptable, while PERSIANN-CDR is poor due to a considerable overestimation of CMA, particularly in southern Hebei and northern Henan. For fRMSE, all RSPPs present similar spatial patterns in mean values, but with significant discrepancies over specific regions (Fig. 3d–f). For example, the southern Henan province has the smallest fRMSE (<0.42) in MSWEP, but the northern Hebei province has the smallest ones in PERSIANN-CDR.

For the study area, the *r* value between the three RSPPs and CMA is 0.93, and all three RSPPs show statistically significant correlations with CMA across the entire region ($p<0.05$), indicating that they can capture the variation of CMA well. However, large spatial discrepancies were found for the three datasets. PERSIANN-CDR and CHIRPS perform better in the northern region ($r>0.95$) than in the south ($r<0.86$), while the performance of MSWEP shows the opposite pattern. KGE of CHIRPS and MSWEP (KGE = 0.88) perform better than PERSIANN-CDR (KGE = 0.86). The optimal skills in the northern, central, and southern of the Huang-Huai-Hai Plain are PERSIANN-CDR, CHIRPS, and MSWEP, respectively. Overall, the three RSPPs can well reproduce the spatial pattern of CMA, but there are large spatial discrepancies. Overall, it is difficult to find one product that has better performance than other products in all areas and for all metrics.

Performance of RSPPs in capturing spatiotemporal variations of SPI

SPI in different time scales

Figure 4 shows the spatial distribution of r value between the three long-term RSPPs and that calculated by CMA. The correlation coefficients between the three long-term RSPPs and CMA also passed the significance test across most regions ($p<0.05$). The larger values of r indicate the better the performance of RSPPs in capturing SPI variation. Over most areas of the Huang-Huai-Hai Plain, the spatial patterns of *r* of the three RSPPs at different time scales are similar with good correlation ($r>0.8$), but some spatial discrepancies are also found in some regions.

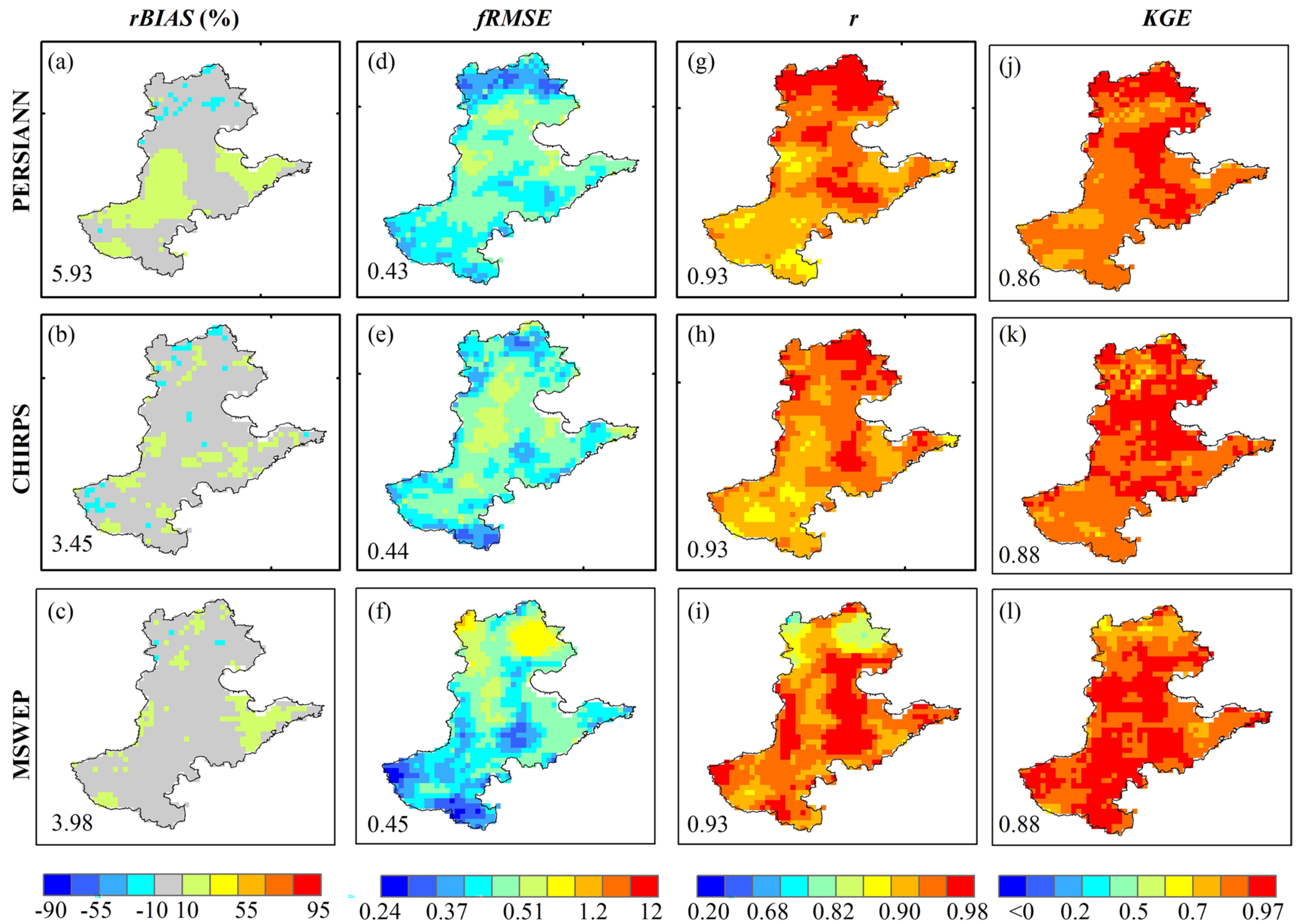

Fig. 3 The spatial distribution of basic metrics for the three long-term RSPPs

For example, in southern Hebei Province, the CHIRPS has poor performance for SPI6 ($r < 0.75$) and SPI12 ($r < 0.68$) (Fig. 4g and h), while in the north of Tianjin, MSWEP has poor skill for SPI6 ($r < 0.70$) and SPI12 ($r < 0.63$) (Fig. 4k and l). Overall, among the three RSPPs, MSWEP has the best estimates of SPI with the closest values to CMA's SPI, followed by PERSIANN-CDR and CHIRPS. For different time scales, *r* of RSPPs generally decreases with the increase of the time scale. For example, for PERSIANN-CDR, the SPI decreased from 0.84 in SPI1 to 0.80 in SPI12, which indicates that relatively short time scales are the optimistic scale for meteorological studies (Gimeno-Sotelo et al. 2024). Therefore, SPI1 is selected for drought event detection and further analysis in our research.

Drought trend and affected area

The interannual fluctuations and affected areas of SPI1 for CMA and RSPPs in the Huang-Huai-Hai Plain are presented in Fig. 5. The SPI1 estimated from RSPPs is highly consistent with that of CMA ($r > 0.95$, $p < 0.05$). They can generally detect the historical extreme drought events from 1983 to 2019 (Fig. 5a). The four most severe drought events captured by the CMA occurred in November 1988, September 1998, February 1999, and May 2001 respectively (shown in Fig. 5a with a shaded area). For the whole region, PERSIANN-CDR performs superior skill in capturing the interannual fluctuations of observational CMA, followed by CHIRPS.

From 1983 to 2019, the fluctuations in the proportion of drought-affected areas detected by RSPPs were consistent with that of CMA (Fig. 5b). The maximum drought-affected area was detected by CMA with a value of 97.6% (November 1988), and the multi-year average area proportion was 16.5%. The three RSPPs underestimated the drought-affected area. Among them, the multi-year average drought area captured by PERSIANN-CDR was 14.9%, but the extreme drought was overestimated in the 1990s; the affected area estimated by CHIRPS was 15.8%, but the extreme drought-affected area was greatly overestimated after 2000. The MSWEP performs superior to the other two products, with the closest value (16.0%) to CMA.

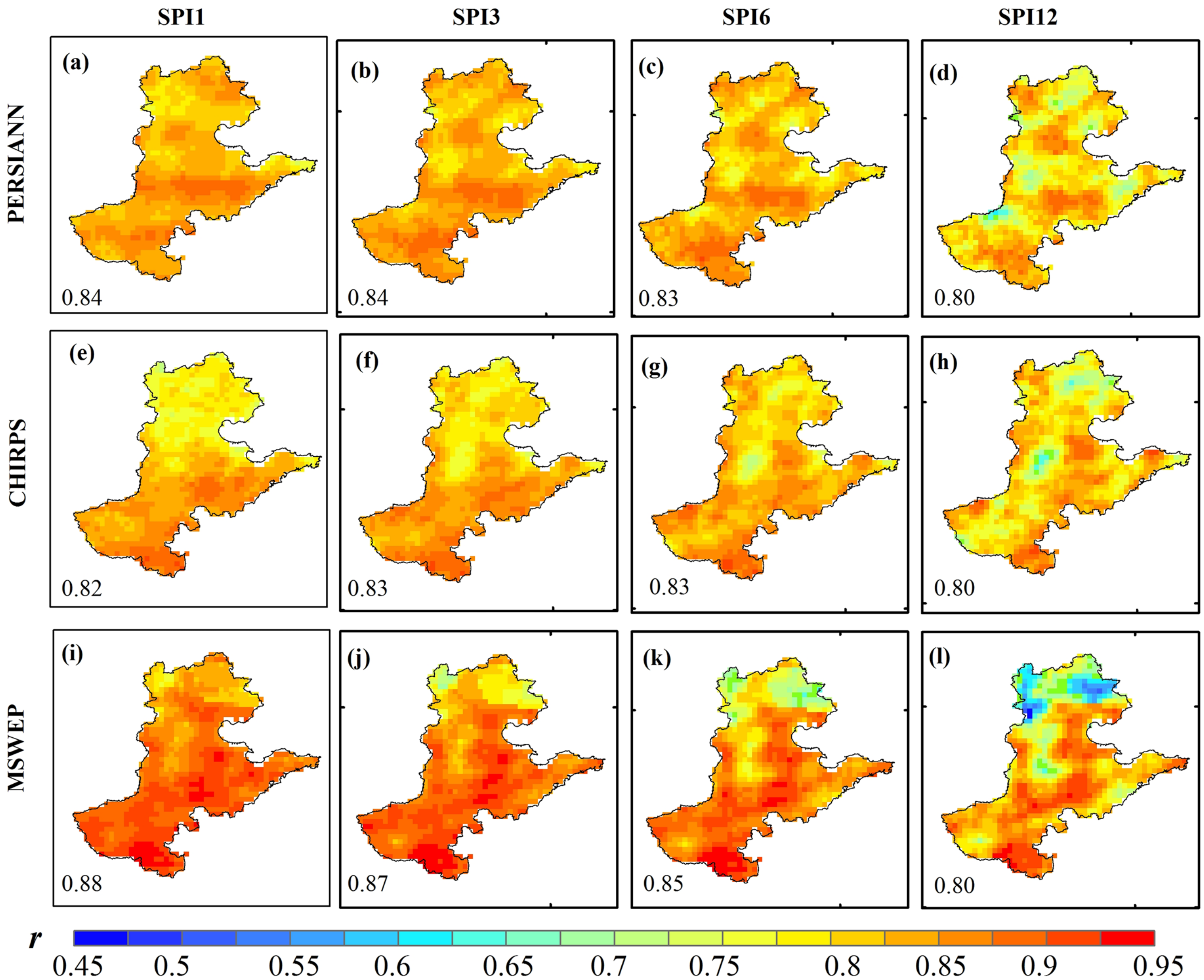

Fig. 4 Spatial pattern of correlation coefficient of SPI calculated by CMA and RSPPs during 1983–2019

Performance of RSPPs in capturing drought events characteristics

Skill in capturing drought categories

The spatial distribution of the performance of three RSPPs in capturing drought category metrics (POD, CSI, and HSS) is presented in Fig. 6. For POD, the overall performance of the three products in the southern region is better than that in the northern region. Among them, MSWEP has the best overall performance (POD = 71.5), followed by PERSIANN-CDR (POD = 59.9) and CHIRPS (POD = 59.6) (Fig. 6d and h). The CSI of MSWEP reached 57.4, especially in eastern Henan Province, eastern and southern Shandong Province (Fig. 6i). At the same time, the CSI performance of PERSIANN-CDR and CHIRPS needs to be improved, with values of 45.9 and 44, respectively (Fig. 6b and e). The HSS value of MSWEP reaches 14.4, especially in the southeastern region of Henan Province, which performs best, where the HSS can reach more than 40 (Fig. 6j), while the PERSIANN-CDR and CHIRPS are only – 4.10 and – 4.58 respectively (Fig. 6c and f).

Overall, regarding the characterization of drought levels, the three metrics of MSWEP are significantly better than those of the other two products, especially HSS and POD. This indicates that among the three RSPPs, MSWEP is the most suitable product for evaluating the drought categories in the Huang-Huai-Hai Plain, and this product is greatly recommended for future studies.

Skill in capturing drought event characteristics

Figure 7 shows the performance of CMA and three RSPPs in capturing drought event characteristics (MDD, MDS,

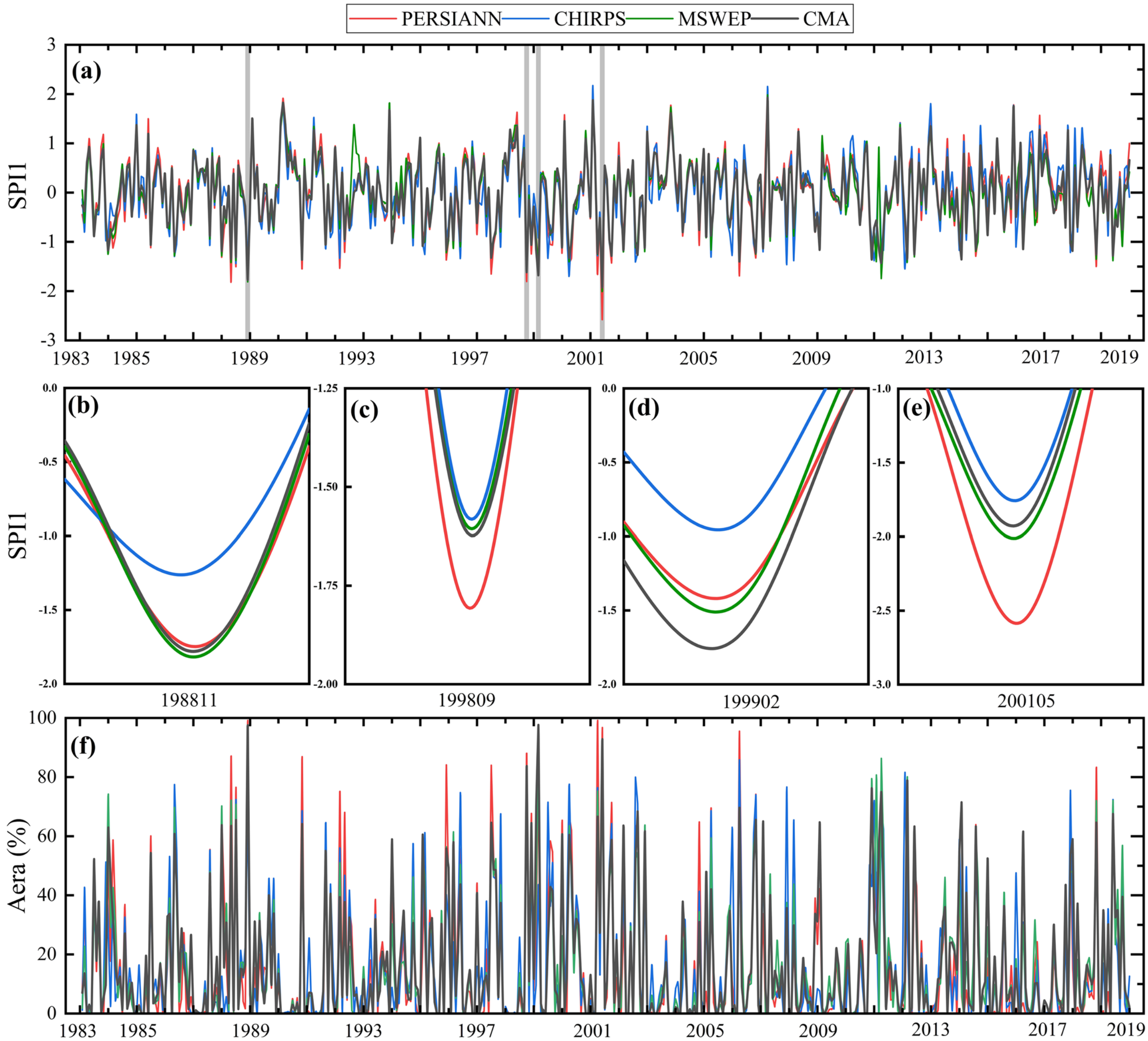

Fig. 5 Drought variation and affected area estimated from CMA and RSPPs during 1983–2019. **b**–**e** are zoomed-in views of the shaded regions in **a**, showing the four most severe drought events captured by CMA

MDI, MDP). For the MDD of CMA, 1.55 months was found in the Huang-Huai-Hai Plain from 1983 to 2019. MDD values below 2 months can be attributed to the inclusion of high-intensity one-month drought events (SPI ≤ – 1.5), which are not ignored in our analysis. Areas with shorter duration of drought events are found in the northwest of Shandong Province and southeastern Hebei Province (MDD < 1.5). In contrast, events with a longer duration are distributed in the central and southern parts of the region (MDD > 1.9) (Fig. 7a). The three RSPPs generally overestimate MDD, among which PERSIANN-CDR overestimates the most seriously (up to 47.7%). MSWEP is the closest to CMA, but they all have severe underestimates in the northern part of Hebei Province (Fig. 7b and d).

The observed MDS is – 1.90, with larger values mainly located in the central and southern regions and low values primarily distributed in the central and northern regions. The mean values of the three RSPPs are generally close to CMA, but they all overestimate in the central part and underestimate in the north and south. In particular, PERSIANN-CDR and MSWEP underestimate drought severity by more than 30% in the north (Fig. 7f–h). The MDI of CMA is – 1.75. All three RSPPs slightly underestimate the drought intensity, which is especially serious in the southern part of the region. However, CHIRPS and MSWEP are

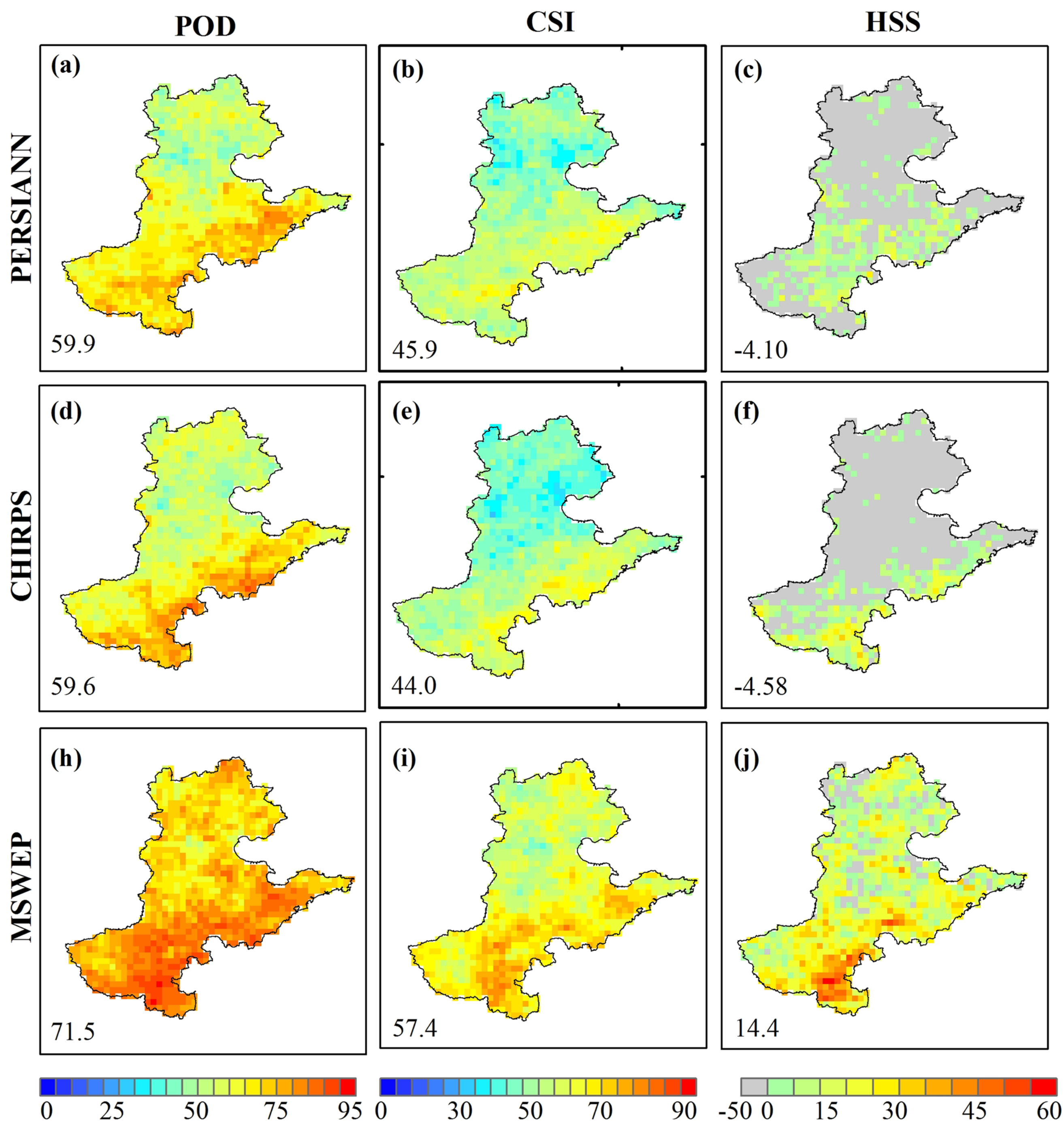

Fig. 6 Spatial distribution of drought categories for three RSPPs

better than PERSIANN-CDR in other regions (Fig. 7lk–l). The average MDP of MSWEP is approximately equivalent to that of CMA (MDP = – 1.86), while PERSIANN-CDR and CHIRPS underestimate the extreme values of drought events, especially severe in the southern region. PERSIANN-CDR and MSWEP perform superiorly in capturing the spatial distribution pattern, but CHIRPS perform poorly (Fig. 7n–p). In summary, it can be seen that among the four drought indicators, the performance of the three RSPPs follows the order of MSWEP > CHIRPS > PERSIANN-CDR.

Performance of RSPPs in capturing specific extreme drought events

We first selected the extreme drought months based on the CMA drought sequence to further assess the three RSPPs'

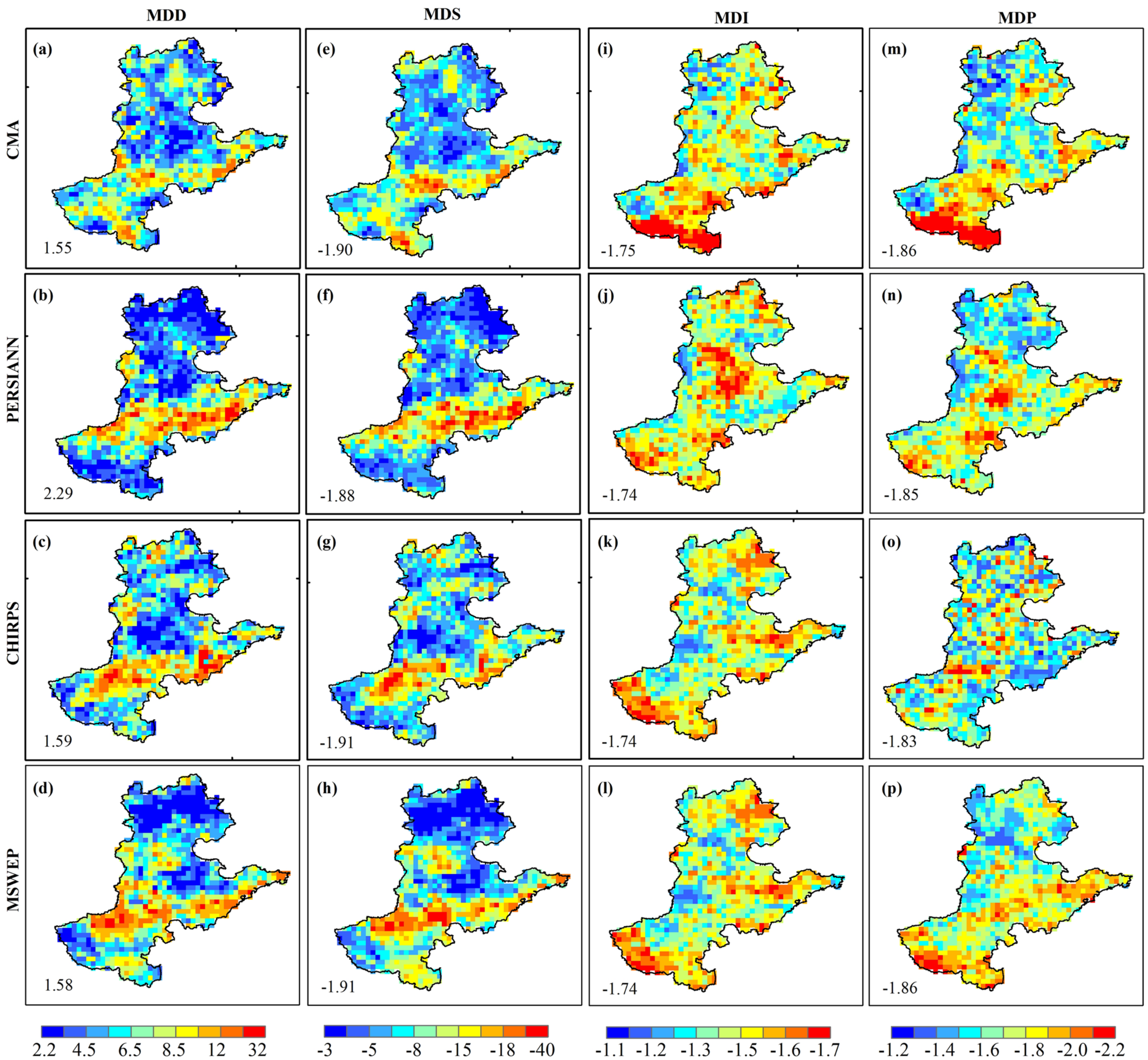

Fig. 7 Spatial distribution of drought events characteristics. Droughts duration, severity, intensity, and peak values are presented in columns 1–4

ability to capture typical extreme drought events in the Huang-Huai-Hai Plain region. Extreme drought months are found in November 1988, September 1998, February 1999, and May 2001, respectively (Fig. 5a). These selected months are used to evaluate the performance of RSPPs in reproducing the spatial distribution of specific extreme drought events. We define SPI = – 1, – 1.5, and – 2 as moderate, severe, and extreme drought.

Although all three RSPPs can identify the drought pattern in November 1988, PERESIANN and CHIRPS underestimated the severity of the drought, especially for CHIRPS (underestimated by 28.7%), while MSWEP slightly overestimated the drought severity, and it can well capture the specific extreme drought events (Fig. 8a–d). For the extreme drought event around September 1998, CMA showed that the extreme drought was generally located in the region's northeast, central, and southeast. Among the three RSPPs, only MSWEP could well capture such a spatial pattern, although it slightly underestimated the severity (Fig. 8e–h). For the third extreme drought event (February 1999), all three RSPPs underestimated the severity of the drought, with PERSIANN-CDR, CHIRPS, and MSWEP underestimating it by 17.9%, 45.7%, and 13.6%, respectively.

The drought event around May 2001 was the most serious, with an average value of – 1.92. Extreme droughts were primarily located in the central and southern areas

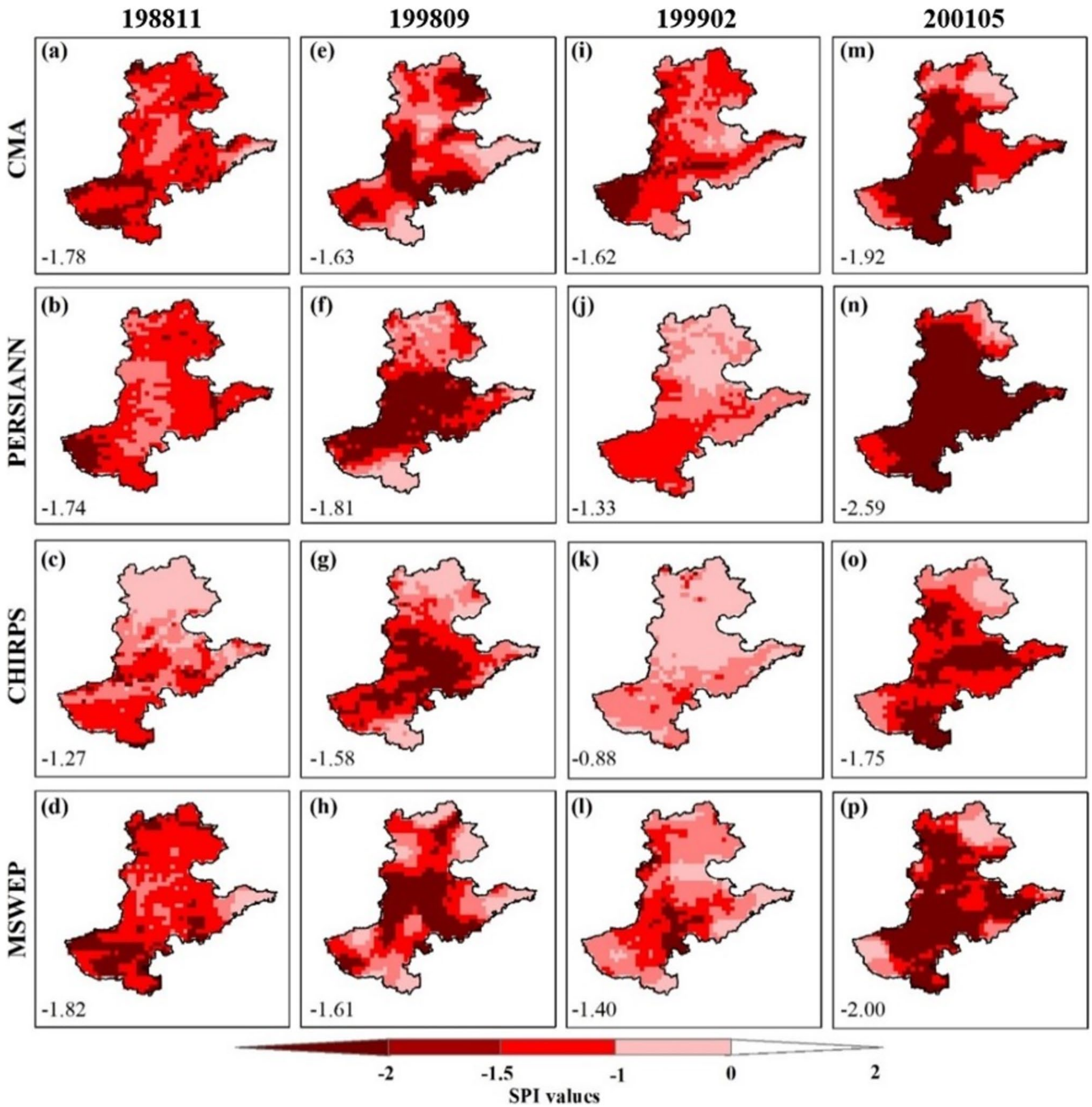

Fig. 8 Spatial distribution of specific extreme drought events calculated from CMA and RSPPs. These extreme events are the most severe drought, as shown in Fig. 5

(accounting for 46.9%). Severe droughts and moderate droughts areas accounted for 31.8% and 14.8%, respectively (Fig. 8m). The regional average of PERSIANN-CDR is – 2.59, overestimating the extent of this drought event (34.9%), of which the extreme drought overestimated by 71.6%. In contrast, CHIRPS underestimates the drought severity by 8.9%, and the extreme drought area is underestimated by 30.6%. Although MSWEP slightly overestimated the severity (4.2%), its mean value was the closest to CMA and had the best skill in capturing the spatial pattern of specific extreme drought (Fig. 8p).

Discussion and uncertainties

Potential factors affecting RSPPs' performance

This study found that MSWEP showed superior performance in terms of basic statistical performance and ability to capture drought event characteristics (Figs. 6, 7, 8). This finding is consistent with previous research (Guo et al. 2022; Li et al. 2022b, 2024; Xu et al. 2019). MSWEP's superior capability stems from its use of the complementary advantages of observation data, microwave remote sensing information, and reanalysis data. Additionally, it conducts bias correction on precipitation on a daily scale, providing relatively reliable precipitation estimates (Beck et al. 2019). CHIPRS and PERSIANN-CDR are slightly inferior to MSWEP in reproducing drought characteristics, mainly because they lack microwave information. Moreover, the CHIRPS is based on the daily scale, which makes it prone to local estimation biases in regions with complex topography, frequent convective precipitation, and sparse observation stations or remote sensing retrievals. In such areas, precipitation exhibits significant spatiotemporal variability over small scales, and interpolation or merging algorithms may struggle to fully capture microtopographic features and convective processes. Therefore, CHIRPS is less suitable for highly spatially heterogeneous and dynamic precipitation environments (Liu et al. 2019). PERSIANN-CDR estimates precipitation based on the statistical relationship between geostationary satellite infrared brightness temperature and rainfall intensity, resulting in a weaker mechanism for retrieving precipitation (Ashouri et al. 2015; Funk et al. 2015).

In addition to the algorithm, terrain significantly affects the performance of RSPPs. For example, in the northern and southwestern regions of our study area, the terrain is complex and diverse (Fig. 1). The ability of the RSPPs to capture drought events is significantly weakened (Fig. 7). This is mainly because precipitation is greatly affected by complex local terrain, making it difficult for remote sensing signals to capture precipitation accurately. Furthermore, these areas are remote and have few observation stations, complicating the verification and improvement of RSPPs retrieval algorithms. Therefore, accurately estimating precipitation in areas with complex terrain or lack of observational data is remains a considerable challenge for accurately calculating precipitation using remote sensing information.

In addition, a comparative analysis between our study and existing studies for drought monitoring over the Huang-Huai-Hai Plain were conducted., and the conclusion highlights the consistencies and discrepancies in detecting drought characteristics across different RSPPs. Zhong et al. (2019) found that CHIRPS and PERSIANN-CDR can effectively capture drought events in typical agricultural areas. However, PERSIANN-CDR shows weaker spatial pattern matching, whereas CHIRPS performs better in identifying the spatial extent and centers of drought events. This result aligns with the advantage of CHIRPS in reproducing spatial distribution characteristics of CMA. Gao et al. (2018) further found CHIRPS's multi-temporal drought monitoring capability in the Hai River Basin. However, they also pointed out that CHIRPS tends to significantly overestimate precipitation in mountainous areas, particularly in regions with high spatial heterogeneity. This finding is consistent with our conclusion that CHIRPS has weaker drought detection capabilities in some areas. In the Yellow River Basin, Wei et al. (2019) found that GPCC 8.0 outperforms PERSIANN-CDR and CHIRPS regarding precipitation consistency, particularly in high-altitude areas where PERSIANN-CDR shows poor drought monitoring performance. However, they observed high consistency (CC > 0.8) among the products in capturing precipitation distribution and drought variations in southeastern regions. In this study, MSWEP demonstrated the best performance in drought monitoring across the Huang-Huai-Hai Plain, consistent with previous findings (Wei et al. 2019), further confirming MSWEP's superior capability in capturing drought variations across different temporal scales.

Overall, the existing literature and our study reveal substantial consistency in drought monitoring performance across different regions while highlighting the limitations of CHIRPS and PERSIANN-CDR in high-altitude or highly heterogeneous areas. This study further emphasizes MSWEP's advantages in monitoring drought categories and extreme drought events, supporting the recommendation to prioritize MSWEP in drought monitoring across the Huang-Huai-Hai Plain. At the same time, it underscores the need to select remote-sensing precipitation products flexibly based on regional characteristics in practical applications.

These extreme drought events are highly consistent with findings from existing literature. Zhong et al. (2019), using SPI3 analysis, reported a prolonged drought in northern China from 1999 to 2000, corresponding to the February 1999 drought event identified in this study. Wang et al. (2015) noted that severe droughts frequently occurred in the 1980s, late 1990s, and early 2000s based on daily SPEI, which validates the regional impacts of the extreme drought events recorded in 1988, 1998, and 2001 in this study. Ali et al. (2020), in their analysis of drought event frequency, found that drought events were more frequent in 2001, aligning with the May 2001 drought event identified in this study. Although these studies used different drought indices and time scales, they point to similar time periods and extreme drought events, indicating that the SPI1-based results in this study are reliable. Furthermore, the complementary nature of different timescale drought indices is demonstrated, suggesting that multi-scale analysis is essential for comprehensive drought monitoring.

Uncertainties and prospective

Although this study has undergone strict quality control, such as the quality control on the observational precipitation data, some uncertainties still inevitably exist. For example, in the calculation of SPI, we use the gamma distribution function to fit the precipitation. However, many fitting functions exist, such as Pearson III type, Weibull type, and log-normal distribution. Previous studies have shown that choosing different theoretical distribution functions significantly impacts drought characteristics. In addition, this study only analyzed the characteristics of the Huang-Huai-Hai Plain and did not comprehensively evaluate the performance of different climate regions and watersheds. However, the conclusions of our study generally follow previous studies, and we confirm the importance of coupling bias correction and microwave information for remote sensing precipitation estimates.

In this study, we validated the performance of three RSPPs in reproducing the drought characteristics. However, all three products require bias correction and processing time before release, with delays from days to months. This time delay limits the application of RSPPs in real-time or near-real-time drought monitoring. However, precipitation estimation at such a time scale has important practical significance for agricultural production and flood forecasting. Therefore, short-time delays or near-real-time RSPPs are urgent to develop in future research. Regarding the issue of "spurious correlation" that may arise from seasonality and time series autocorrelation, this study mainly relies on monthly-scale data spanning over 30 years, which to some extent smooths out the impact of seasonal fluctuations. However, given that the core objective of this study focuses on the comparative evaluation of multi-source precipitation products, more rigorous detrending processes have not yet been applied. Future research could implement stricter raw data processing to minimize potential spurious correlation effects.

It is worth noting that this study's evaluation of the spatiotemporal distribution of droughts and the identification of extreme events using multi-source remote sensing precipitation products not only helps to understand the performance differences of RSPPs but also provides valuable references for agricultural planning and drought prevention in the Huang-Huai-Hai Plain and similar regions. On the one hand, timely identification of drought periods and areas can facilitate precise irrigation and rational water resource allocation, avoiding resource waste. On the other hand, for drought-prone or precipitation-sensitive regions, the drought frequency characteristics captured in this study can guide the selection of drought-tolerant crop varieties and adjustments to planting structures. Furthermore, analyzing extreme drought events offers direct scientific support for government departments in formulating drought emergency plans and long-term food security strategies, particularly in mitigating disaster risks during critical agricultural periods.

Conclusions

In this study, using the SPI and run theory, we quantitatively evaluated the capability of three long-term RSPPs (PERSIANN-CDR, CHIRPS, and MSWEP) in detecting drought characteristics over the Huang-Huai-Hai plain. The main conclusions are as follows:

(1) Significant discrepancies were found among the different RSPPs in characterizing the precipitation of CMA. The three RSPPs generally captured the spatial pattern of the annual average of CMA, but overestimated the annual mean precipitation, by 6.0%, 3.6%, and 3.6% for PERSIANN-CDR, CHIRPS, and MSWEP, respectively. CHIRPS showed the best performance in terms of rBIAS, fRMSE, r, and KGE, followed by MSWEP and PERSIANN-CDR.

(2) MSWEP reasonably estimated the variations of CMA's SPI, followed by PERSIANN-CDR, and CHIRPS. For different time scales, the correlation coefficient (*r)* of the three RSPPs generally decreased as the time scale increased, with the one-month scale (SPI1) showing the best consistency. In terms of monitoring drought fluctuation (SPI1) over time, PERSIANN-CDR performed best and was relatively consistent with the changing trend of CMA. In estimating the proportion of drought area, MSWEP has the best overall performance, followed by PERSIANN-CDR and CHIRPS.

(3) Regarding evaluating drought categories, MSWEP performed at a superior level compared to the other two products, especially in HSS and POD. For the characteristics of drought events described by MDD, MDS, MDI, and MDP, MSWEP performs best, followed by CHIRPS and PERSIANN-CDR. In capturing the spatial distribution of the specific extreme drought events, MSWEP performs well, while CHIRPS performs poorly. Thus, all three products still have much room for improvement in drought monitoring.

Acknowledgements We sincerely appreciate the reviewers' valuable comments and suggestions, which have greatly improved the quality of this manuscript.

Author contributions P.N.H. guided, reviewed, and revised this manuscript. M.J.H. wrote the main manuscript text. A.Q.F. guided the framework and provided funding. Y.Z.L. reviewed and revised the text and figures. K.X.Y. gives suggestions to the revised manuscript. All authors have reviewed the manuscript.

Funding This research was jointly funded by the Belt and road Fund on Water and Sustainability of The National Key Laboratory of Water Disaster Prevention (2023490111, 2023490711), Open Research Fund Program of State Key Laboratory of Eco-hydraulics in Northwest Arid Region, Xi'an University of Technology (2023KFKT-1), and the National Key R&D Program of China (2023YFC3206801).

Data availability The daily precipitation data are available from the National Meteorological Information Center of China at http://data.cma.cn/. The three long-term remote sensed precipitation productions can be obtained from three sources: (1) national centers of environmental information (https://www.ncei.noaa.gov/data/-precipitation-persiann/access/); (2) Climate Hazards Center of University of California (https://data.chc.ucsb.edu/products/); (3) Department of Civil and Environmental Engineering of Princeton University (https://www.gloh2o.org/mswx/). Spatial figures were created by ArcGIS 12.7. Code for processing the datasets can be available on request.

Declarations

Conflict of interest The authors declare no competing interests.

References

AghaKouchak A, Farahmand A, Melton FS et al (2015) Remote sensing of drought: progress, challenges and opportunities. Rev Geophys 53(2):452–480

Ali R, Kuriqi A, Kisi O (2020) Human–environment natural disasters interconnection in China: a review. Climate 8(4):48

Ashouri H, Hsu K-L, Sorooshian S et al (2015) PERSIANN-CDR: daily precipitation climate data record from multisatellite observations for hydrological and climate studies. Bull Am Meteor Soc 96(1):69–83

Beck HE, Wood EF, Pan M et al (2019) MSWEP V2 global 3-hourly 0.1° precipitation: methodology and quantitative assessment. Bull Am Meteorol Soc 100(3):473–500

Brito CS, Silva RM, Santos CAG et al (2021) Monitoring meteorological drought in a semiarid region using two long-term satellite-estimated rainfall datasets: a case study of the Piranhas River basin, northeastern Brazil. Atmos Res 250:105380

Ebert EE, Janowiak JE, Kidd C (2007) Comparison of near-real-time precipitation estimates from satellite observations and numerical models. Bull Am Meteor Soc 88(1):47–64

Fleig AK, Tallaksen LM, Hisdal H et al (2006) A global evaluation of streamflow drought characteristics. Hydrol Earth Syst Sci 10(4):535–552

Funk C, Peterson P, Landsfeld M et al (2015) The climate hazards infrared precipitation with stations: a new environmental record for monitoring extremes. Sci Data 2(1):150066

Gao F, Zhang Y, Ren X et al (2018) Evaluation of CHIRPS and its application for drought monitoring over the Haihe River Basin, China. Nat Hazards 92:155–172

Gimeno-Sotelo L, Sorí R, Nieto R et al (2024) Unravelling the origin of the atmospheric moisture deficit that leads to droughts. Nat Water 2(3):242–253

Guo H, Bao A, Liu T et al (2017) Meteorological drought analysis in the lower Mekong basin using satellite-based long-term CHIRPS product. Sustainability 9(6):901

Guo H, Li M, Nzabarinda V et al (2022) Assessment of three long-term satellite-based precipitation estimates against ground observations for drought characterization in Northwestern China. Remote Sens 14(4):828

Huffman GJ, Bolvin DT, Braithwaite D et al (2015) NASA global precipitation measurement (GPM) integrated multi-satellite retrievals for GPM (IMERG). 4(26):30

Hutchinson MF, Xu T (2004) Anusplin version 4.2 user guide, Centre for Resource Environmental Studies, The Australian National University, Canberra

Joyce RJ, Janowiak JE, Arkin PA et al (2004) CMORPH: a method that produces global precipitation estimates from passive microwave and infrared data at high spatial and temporal resolution. J Hydrometeorol 5(3):487–503

Li M, Lv X, Zhu L et al (2022a) Evaluation and application of MSWEP in drought monitoring in Central Asia. Atmosphere 13(7):1053

Li Y, Zhuang J, Bai P et al (2022b) Evaluation of three long-term remotely sensed precipitation estimates for meteorological drought monitoring over China. Remote Sens 15(1):86

Li Y, Yan H, Chen L et al (2024) Performance and uncertainties of five popular satellite-based precipitation products in drought monitoring for different climate regions. J Hydrol 628:130562

Liu S, Mo X, Lin Z et al (2010) Crop yield responses to climate change in the Huang-Huai-Hai Plain of China. Agric Water Manag 97(8):1195–1209

Liu J, Shangguan D, Liu S et al (2019) Evaluation and comparison of CHIRPS and MSWEP daily-precipitation products in the Qinghai-Tibet Plateau during the period of 1981–2015. Atmos Res 230:104634

Ma F, Yuan X (2023) When will the unprecedented 2022 summer heat waves in Yangtze River Basin become normal in a warming climate? Geophys Res Lett 50(4):e2022

McKee TB, Doesken NJ, Kleist J (1993) The relationship of drought frequency and duration to time scales, California. pp 179–183

Schaefer JT (1990) The critical success index as an indicator of warning skill. Weather Forecast 5(4):570–575

Sreeparvathy V, Srinivas VV (2022) A Bayesian fuzzy clustering approach for design of precipitation gauge network using merged remote sensing and ground-based precipitation products. Water Resour Res 58(2):1–33

Sternberg T, Thomas D, Middleton N (2011) Drought dynamics on the Mongolian steppe, 1970–2006. Int J Climatol 31(12):1823–1830

Su B, Huang J, Fischer T et al (2018) Drought losses in China might double between the 1.5 °C and 2.0 °C warming. Proc Natl Acad Sci 115(42):10600–10605

Sun Q, Miao C, Duan Q et al (2018) A review of global precipitation data sets: data sources, estimation, and intercomparisons. Rev Geophys 56(1):79–107

Tuan NT, Qiu J-J, Verdoodt A et al (2011) Temperature and precipitation suitability evaluation for the winter wheat and summer maize

cropping system in the Huang-Huai-Hai plain of China. Agric Sci China 10(2):275–288
Wang Q, Shi P, Lei T, Geng G, Liu J, Mo X, Wu J (2015) The alleviating trend of drought in the Huang-Huai-Hai Plain of China based on the daily SPEI. Int J Climatol 35(13):3760–3769
Wei L, Jiang S, Ren L et al (2019) Performance of two long-term satellite-based and GPCC 8.0 precipitation products for drought monitoring over the Yellow River Basin in China. Sustainability 11(18):4969
Wilks DS (2011) Statistical methods in the atmospheric sciences. Academic press Inc., London
Xie J, Liu X, Jasechko S et al (2024) Majority of global river flow sustained by groundwater. Nat Geosci 17(8):770–777
Xu Z, Wu Z, He H et al (2019) Evaluating the accuracy of MSWEP V2.1 and its performance for drought monitoring over mainland China. Atmos Res 226:17–31
Yuan X, Wang Y, Ji P et al (2023) A global transition to flash droughts under climate change. Science 380(6641):187–191
Zargar A, Sadiq R, Naser B et al (2011) A review of drought indices. Environ Rev 19:333–349
Zhang Y, Zheng H, Zhang X et al (2023) Future global streamflow declines are probably more severe than previously estimated. Nat Water 1(3):261–271
Zhong R, Chen X, Lai C et al (2019) Drought monitoring utility of satellite-based precipitation products across mainland China. J Hydrol 568:343–359